

Monitoring fine-grained soils loading with Time-Domain Reflectometry

Faroqy, Anna; Royal, Alexander; Curioni, Giulio; Chapman, David; Cassidy, Nigel

DOI:

[10.1061/\(ASCE\)GT.1943-5606.0002253](https://doi.org/10.1061/(ASCE)GT.1943-5606.0002253)

License:

Other (please specify with Rights Statement)

Document Version

Peer reviewed version

Citation for published version (Harvard):

Faroqy, A, Royal, A, Curioni, G, Chapman, D & Cassidy, N 2020, 'Monitoring fine-grained soils loading with Time-Domain Reflectometry', *Journal of Geotechnical and Geoenvironmental Engineering - ASCE*, vol. 146, no. 6, 04020036. [https://doi.org/10.1061/\(ASCE\)GT.1943-5606.0002253](https://doi.org/10.1061/(ASCE)GT.1943-5606.0002253)

[Link to publication on Research at Birmingham portal](#)

Publisher Rights Statement:

This material may be downloaded for personal use only. Any other use requires prior permission of the American Society of Civil Engineers. This material may be found at <https://ascelibrary.org/doi/10.1061/%28ASCE%29GT.1943-5606.0002253>

General rights

Unless a licence is specified above, all rights (including copyright and moral rights) in this document are retained by the authors and/or the copyright holders. The express permission of the copyright holder must be obtained for any use of this material other than for purposes permitted by law.

- Users may freely distribute the URL that is used to identify this publication.
- Users may download and/or print one copy of the publication from the University of Birmingham research portal for the purpose of private study or non-commercial research.
- User may use extracts from the document in line with the concept of 'fair dealing' under the Copyright, Designs and Patents Act 1988 (?)
- Users may not further distribute the material nor use it for the purposes of commercial gain.

Where a licence is displayed above, please note the terms and conditions of the licence govern your use of this document.

When citing, please reference the published version.

Take down policy

While the University of Birmingham exercises care and attention in making items available there are rare occasions when an item has been uploaded in error or has been deemed to be commercially or otherwise sensitive.

If you believe that this is the case for this document, please contact UBIRA@lists.bham.ac.uk providing details and we will remove access to the work immediately and investigate.

1 Monitoring fine-grained soils loading with Time- 2 Domain Reflectometry

3
4 **Authors:**

5
6 **Faroqy, A.¹, Royal, A.C.D.², Curioni, G.³, Chapman, D.N.⁴, Cassidy, N.J.⁵**

7
8
9 ¹Dr Anna Faroqy*, Department of Civil Engineering, School of Engineering, University of Birmingham,
10 Edgbaston, Birmingham, B15 2TT, United Kingdom

11 ²Dr Alexander C.D. Royal, Department of Civil Engineering, School of Engineering, University of
12 Birmingham, Edgbaston, Birmingham, B15 2TT, United Kingdom

13 ³Dr Giulio Curioni, School of Geography, Earth & Environmental Sciences, University of Birmingham,
14 Edgbaston, Birmingham, B15 2TT, United Kingdom

15 ⁴Prof. David N. Chapman, Department of Civil Engineering, School of Engineering, University of
16 Birmingham, Edgbaston, Birmingham, B15 2TT, United Kingdom

17 ⁵Prof. Nigel J. Cassidy, Department of Civil Engineering, School of Engineering, University of
18 Birmingham, Edgbaston, Birmingham, B15 2TT, United Kingdom

19
20
21
22
23
24 * Corresponding author: Anna Faroqy, Department of Civil Engineering, University of Birmingham,
25 Edgbaston, Birmingham, B15 2TT, United Kingdom. Tel.: +44 01214143564, email:
26 a.faroqy@bham.ac.uk
27

28 **Abstract**

29 Subsurface geophysical investigations have the potential of providing information for the long-term
30 monitoring of geotechnical assets. This research evaluates the suitability of vertically and horizontally
31 orientated, embedded Time Domain Reflectometry (TDR) measurements for monitoring of near-
32 saturated, fine-grained soils under vertical loading conditions. TDR measurements were carried out
33 regularly during vertical loading and unloading of near- and fully-saturated soil mixtures containing
34 fine-sand, kaolinite and bentonite. The results show that TDR probe orientation, in relation to the load
35 direction, affects the values of TDR-measured apparent permittivity (AP) and bulk electrical
36 conductivity (BEC). The relationship between the soil void ratio and AP was found to be clearer when
37 measured in the direction of loading whereas AP and BEC measured normal to the load application
38 appears to reflect changes in pore-water pressure. BEC was found to be more variable and less
39 obvious. It is concluded that monitoring relative changes in temporal AP and BEC using embedded TDR
40 sensors can provide unique and valuable information on how a soil responds to loading under near-
41 saturated conditions.

42
43 **Keywords:** Time Domain Reflectometry, geophysical monitoring, saturated soils, ground
44 investigation, geotechnical asset, TDR probe orientation

45

46 Introduction

47 Geotechnical asset failures can lead to catastrophic consequences. Earth dam failures alone caused
48 the loss of thousands of lives globally (Charles et al., 2011). Therefore, there is a pressing need for
49 improved, long-term monitoring, management and planned interventions strategies for key
50 infrastructure assets (Clarke et al., 2016). Long-term asset monitoring is still not common practice
51 (Shah, 2014) as it often requires high initial investment and special technical expertise for the
52 management of the instrumentation and data collected. Nonetheless, there has been a considerable
53 drive in the geotechnical community to improve the nature, accuracy and cost of asset monitoring
54 systems (Basu et al., 2013) with geophysical methods being increasing popular (McDowell et al., 2002).
55 Geophysical monitoring has several benefits over traditional ground investigation methods as it
56 captures the temporal changes in soil behaviour and is able to capture trends in ground deformation
57 (Rogers et al., 2012). Given that many of the physico-chemical factors affecting the engineering
58 behaviour of soils also affect their electrical response (Schön, 2004), non-intrusive electrical-based
59 geophysical sensing techniques have been the focus of significant research effort in the past decade
60 (e.g., Lambot et al., 2009; Royal et al., 2011). Ground-Penetrating Radar, Electrical Resistivity Imaging
61 and Electromagnetic Induction are all common non-invasive geophysical techniques that utilise
62 changes in the electrical properties of the ground (i.e., permittivity and conductivity) to infer
63 geotechnical behaviour. To be of value for long-term geotechnical asset monitoring, it is important
64 that the interpreted geophysical parameters are reliably and consistently related to the *in-situ*
65 geotechnical properties, such as gravimetric water content (GWC) and dry density (ρ_d). Time Domain
66 Reflectometry (TDR) is a relatively inexpensive sensing technique that can achieve this (Curioni et al.,
67 2018a) and although it has been an active research area in unsaturated soil monitoring (e.g. Mojid et
68 al., 2003; Ekblad and Isacsson, 2007; Curioni et al., 2018b), its response in saturated and near-
69 saturated ground conditions has not been studied extensively. Nonetheless, the relationship between
70 TDR-measured apparent permittivity (AP) and void ratio (e) measured in an oedometer (Liu, 2007), as

71 well as its application in the prediction of ground settlement (Janik et al., 2017), show that TDR
72 techniques can be used for the effective monitoring of saturated and near-saturated soils.

73 TDR probes require embedding into the medium being investigated and although probe orientation
74 has been suggested as a factor affecting volumetric water content (VWC) estimation (Skierucha et al.,
75 2004; Pastuszka et al., 2014), to date, no research has addressed the relationship between probe
76 orientation and its influence on the measured AP and BEC under vertical loading conditions. As such,
77 the purpose of this paper is to:

78 (i) investigate whether TDR can be used to effectively monitor temporal changes in near-saturated
79 fine-grained soils of varying plasticity that are subject to vertical loading, and to

80 (ii) evaluate whether TDR probe orientation significantly affects AP and BEC readings during
81 controlled, laboratory experiments of loading and un-loading of these soils.

82 The overall aim of the research is to provide, for the first time, reliable information on the sensitivity
83 of TDR probe orientation to the observed values of measured AP and BEC in saturated materials and
84 how this reflects changes in the geotechnical behaviour of fine-grained soils. More specifically, to
85 show how the relationship of embedded electrical properties measured by TDR can be used to
86 'ground-truth' non-invasive geophysical data and improve the interpretation of time-lapse
87 geophysical monitoring surveys for key geotechnical assets. This will be discussed on the basis of the
88 results of experimental laboratory testing carried out during vertical loading and unloading of near-
89 and fully-saturated soil mixtures including varied proportions of fine-sand, kaolinite and bentonite.

90

91 ***Background***

92 TDR probe measurements have been known predominately for the estimation of VWC in unsaturated
93 soils based on its relationship with AP (Topp et al., 1980). Its high accuracy (VWC within 1-2% - Jones
94 et al., 2002), when calibrated to specific soil conditions, GWC within $\pm 2\%$ and $\rho_d \pm 5\%$ under
95 laboratory conditions (Curioni et al., 2018b), in addition to the possibility of automated remote control

96 (Mitchell and Liu, 2006) makes TDR a reliable and accurate soil monitoring tool. Considering TDR's
 97 application in ground investigation only in the context of its VWC estimation capability, might have
 98 led to a general perception that TDR is unreliable when used in high water and high clay content soils.
 99 Whilst VWC cannot be accurately estimated in soils with GWC exceeding approximately 55% with the
 100 most commonly applied Topp's equation (Topp et al., 1980), it is possible to measure AP and BEC at
 101 higher water contents (e.g. Thomas et al., 2010). However, high clay contents, leading to high BEC
 102 values and high signal attenuation, can compromise the ability of TDR to effectively characterise soil's
 103 electrical parameters. The 'BEC threshold' is dependent on the probe length (Heimovaara, 1990), for
 104 example, waveform measurements with 45 mm long rods were found to be detrimentally attenuated
 105 at BEC values above 0.3 S/m (Mojid et al., 2003). (Further information regarding AP and BEC
 106 determination from TDR signal can be found, for example, in Jones et al., (2002), and Cassidy, (2009)).
 107 Experiments conducted by Liu, (2007) in saturated fine-grained soils, at the end of the oedometer
 108 consolidation stages, showed a positive correlation between AP and void ratio, e. Meanwhile, BEC
 109 measured at the end of subsequent consolidation stages decreased with fluid expulsion in some clays,
 110 but in others exhibited a negligible change (Liu, 2007). Furthermore, earth dam settlement prediction
 111 based on AP measurements was achieved with an accuracy of 19% (Janik et al., 2017), illustrating the
 112 potential of TDR technique for the *in-situ* investigation of saturated soils.
 113 In fully saturated soils, the geotechnical parameters of VWC (Equation 1), GWC (Equation 2) and ρ_d
 114 (Equation 3) can be determined from the estimated value of e.

115

$$VWC = \frac{e}{1 + e} \quad (m^3/m^3) \quad \text{Equation 1}$$

$$GWC = VWC \frac{\rho_w}{\rho_d} \quad (kg/kg) \quad \text{Equation 2}$$

$$\rho_d = \frac{m_s}{V} \quad (kg/m^3) \quad \text{Equation 3}$$

116

117 where ρ_w is the density of water (assumed as 1000 kg/m³ at 4°C) and ρ_d is estimated from the initial
118 dry mass solids (m_s) and the specimen volume (V). The determination of e during 1D consolidation
119 can then lead to estimation of soil compressibility from the compression index (C_c) based on the
120 correlation between e and the log of effective stress (Terzaghi et al., 1996).

121 TDR probe orientation was indicated as an important factor in the estimation of VWC by Skierucha et
122 al., (2004) and Pastuszka et al., (2014). In the materials having uniform porosity, grain size and shape,
123 such as glass beads, TDR results are expected to be nearly the same in any direction, apart from minor
124 discrepancies that can arise from the water distribution along the rods (Jones and Friedman, 2000). In
125 layered, porous, saturated materials (where water level changes are perpendicular to a vertically
126 orientated TDR probe) - Robinson et al., (2003) and Pastuszka et al., (2014) concluded that the
127 vertically inserted probe represents the arithmetic mean of soil moisture for the investigated depth.
128 Conversely, horizontally inserted probes reflect the water content of a single layer at a specific depth.
129 Jones and Friedman (2000) reported that the vertically measured AP (AP_v) could be twice as higher as
130 the horizontally measured AP (AP_h) in soils containing platy particles. However, this result could be
131 affected by the particular experimental arrangement used in the study. To date, no research has
132 attempted to link the effect of TDR probe orientation on its AP and BEC readings in fine-grained soils
133 under a vertical loading.

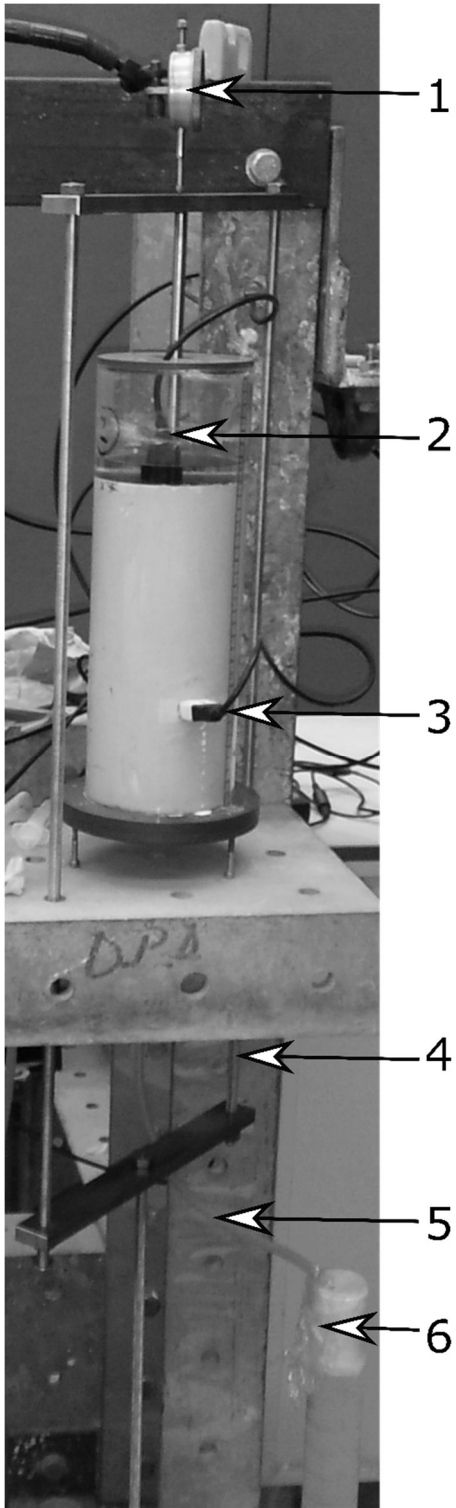
134 **Experimental Methodology**

135 ***TDR in vertical loading - apparatus***

136 A bespoke apparatus was built to test the AP and BEC response from TDR probes located in both the
137 direction of loading and normal to it. The vertical loading test arrangement (Figure 1) included a
138 Perspex consolidation chamber with two TDR probes and a dead-weight loading system. The TDR
139 apparatus comprised a Campbell Scientific TDR100 operated via the proprietary PCTDR software and
140 CS645 probes (three-rod, 75 mm long, with rod diameters and separations of 1 mm and 5 mm

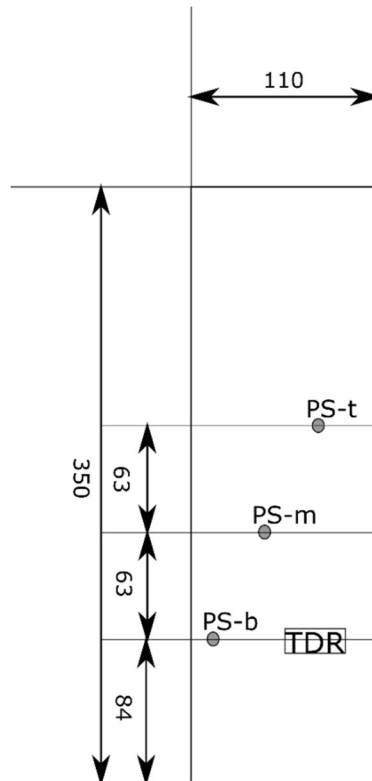
141 respectively) with a 3 m long coaxial cable. Three identical chambers were constructed, each with an
142 inner diameter of 110 mm and height of 300 mm. The dimensions were designed to minimise the
143 boundary effect on the consolidation process and account for the zone of influence of the TDR probes
144 (Mojid et al., 2003). Drainage was facilitated at the top and bottom of the specimen with perforated
145 plastic plates covered with filter paper within the chamber. Two TDR probes were installed
146 perpendicularly to each other; one (TDR_v) mounted vertically in the direction of loading in the middle
147 of the top drainage plate and the other (TDR_h) installed horizontally and fitted into the chamber wall
148 at the height of 83 mm from the base, Figure 1. Additionally, one of the chambers was instrumented
149 with external pore-water pressure sensors positioned at three depths: at the height of TDR_v (PS-t), in
150 the middle of the specimen (PS-m) and at the same height as TDR_h (PS-b), Figure 2.

151



152

153 **Figure 1. TDR chamber set-up under load conditions: 1 - compression gauge, 2- vertical TDR probe,**
154 **3 - horizontal TDR probe, 4 - loading frame, 5 - bottom drainage pipe, 6 - drainage container.**



155

156 **Figure 2. Schematic of the TDR chamber equipped with the pore pressure sensors (PS), positioned**
 157 **at the bottom (b), middle (m) and top (t) of the chamber, measurements in mm**

158

159 The soil specimens were prepared at a range of water contents, between 1 to 1.8 times the liquid limit
 160 (LL), and were subjected to a gradual load increase from 5 kPa to a maximum 160 kPa and unload (the
 161 load increments varied in different samples and are provided in Table 2). The load was applied using
 162 dead weights supported on hangers that rested on the top of a metal bar mounted perpendicular to
 163 the top drainage plate (Figure 1). During each load increment, the change in the specimen height (and
 164 associated time) was recorded to calculate the time-dependant settlement parameters following the
 165 oedometer test procedure (BSI, 1990b).

166 In standard oedometer tests, an equal pressure head is maintained at the top and bottom of the
 167 specimen to maintain hydrostatic conditions. In the design of the TDR chambers, it was not possible
 168 to place the specimen in a water bath, due to the presence of the TDR probes. In order to equalise the
 169 pressure head, filling the bottom drainage pipe with water to the level of the top drainage plate was
 170 initially considered. However, adding water to the drainage pipe would have diluted the pore fluid

171 and, as such, preclude the chemical and electrical investigation of its properties (which was deemed
172 more important than maintaining hydrostatic conditions). Therefore, whilst the upper and lower
173 drains were used in the chambers, the water in each was not at the same head. The fluid dripping out
174 of the bottom drain was collected in a container approximately 1 m below the bottom of the chamber
175 (suggesting that the lower head, at the base of the chamber, was equivalent to atmospheric pressure
176 and was effectively constant). Pore fluid seeping out of the upper face of the specimen accumulated
177 on top of the perforated loading plate, slightly increasing the magnitude of the upper head acting
178 upon the specimen.

179 The physical set-up of the experiment precluded the use of a slip lining between the chamber wall and
180 the soil. Consequently, soil located near the base of the chamber was not expected to experience a
181 significant proportion of the vertical load applied as frictional forces between the chamber and
182 specimen were expected to dominate with depth (Olson, 1986). The exact extent of the friction effect
183 could not be measured directly with this chamber.

184 ***TDR data acquisition***

185 TDR measurements were taken at a range of consolidation times. Measured signal travel time and
186 reflection coefficient, were used to compute the AP and BEC using the tangent method and the long
187 distance steady-state reflections respectively (Heimovaara and Bouten, 1990; Huisman et al., 2008),
188 following the code developed by Curioni et al. (2012). The equations underlying AP and BEC estimation
189 from TDR signal are included below for the ease of reference, nonetheless further details regarding
190 the calibration procedure can be found in Faroqy (2018) or Curioni et al., 2018.

191 AP was computed using Equation 4:

$$AP = \left(\frac{l_a}{L}\right)^2 \quad \text{Equation 4}$$

192 where L is TDR probe length, ($l_a = \frac{ct}{2}$) - apparent length, c - the speed of light in free space ($2.988 \times$
193 10^8 m/s), and t/2 - a time for the signal's travel down and back.

194 BEC was obtained from Equation 5:

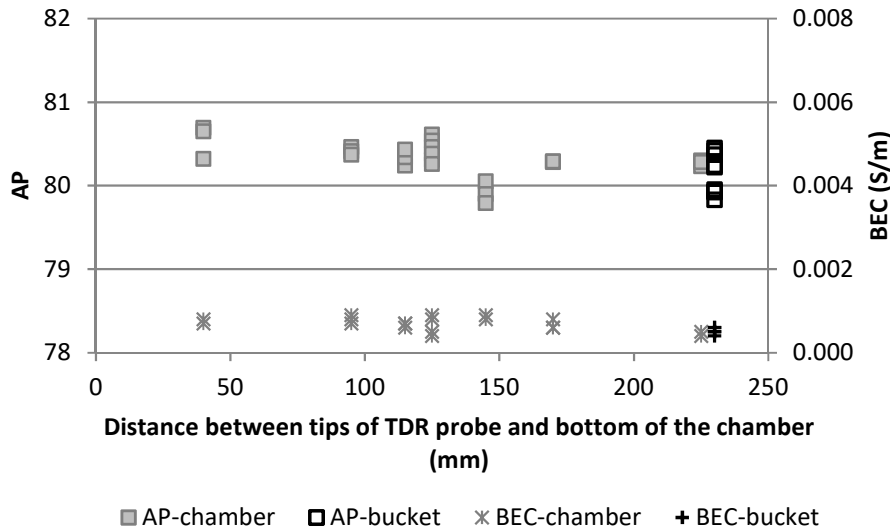
$$BEC = \frac{K_p}{R_l - (DR_c + R_0)} \quad \text{Equation 5}$$

195 Where (K_p) (1/m) is the probe constant, R_c and R_0 (Ω) – resistance corresponding to the
196 transmission-line elements other than the probe (i.e. the TDR unit, cable and connectors), D - cable
197 length (m), and R_l - load resistance (Ω),

$$R_l = Z_{out} \frac{1 + \rho_{\infty}}{1 - \rho_{\infty}}$$

198 Where Z_{out} is the output impedance of the TDR device (i.e. 50 Ω) and ρ_{∞} is the reflection coefficient
199 taken at long distances, when all the multiple reflections have attenuated and the signal has reached
200 a steady-state level. The TDR frequency bandwidth was expected to be between 100 MHz and 500
201 MHz (Robinson et al., 2003).

202 Prior to the consolidation testing, the TDR probes were calibrated in air, water and saline solutions
203 (0.0063-1.7960 S/m) following Heimovara (1993) and Huisman et al., (2008). To ensure that the
204 measurements were not affected by the container and/or the localised presence of two probes, AP
205 and BEC readings were obtained in de-ionised water (BEC~ 0.0009 S/m) within the chamber and a
206 larger container with the vertical probe at the different heights. The results indicated that the
207 container size and the position of the vertical probe relative to the horizontal probe in the experiment
208 did not affect the TDR readings (Figure 3).



209

210 **Figure 3. TDR measurements taken in DI water in the chamber and larger bucket to investigate the**
 211 **container effect on the measurements**

212 Significant changes in temperature can impact upon the derived TDR data, as well as the physical
 213 properties of the soil (Mitchell and Soga, 2005). In the laboratory experiments, temperature
 214 measurements were collected every 15 minutes in air and inside each chamber with an automated
 215 LM-35 probe with an accuracy of 0.5°C (Sadeghioon et al., 2014). Conditions were generally stable at
 216 a temperature of 20°C with minimum and maximum values of 15-25°C, respectively.

217 Based on previous literature (Thring et al., 2014, Jung et al. 2013b), it was deemed that this range of
 218 temperatures had a negligible effect on AP, whilst its effect on the BEC was accounted for by applying
 219 a temperature correction factor according to Equation 6, (Keller and Frischknecht, 1966).

$$BEC_T = \frac{BEC_{uncor}}{1 + \alpha (T - T_{uncor})} \quad \text{Equation 6}$$

220 where BEC_T and BEC_{uncor} are the corrected and measured BEC at a certain temperature T_{uncor} ,
 221 respectively, T is the reference temperature (20°C), and α is a correction factor (in this study, 0.025,
 222 based on Abu-Hassanein et al., (1996)).

223 ***Soils used in the investigation and their geotechnical properties***

224 The vertical loading tests were conducted on three soil mixtures prepared from commercially available
225 English China Clay, sodium activated bentonite, and kiln dry fine sand.

226 Mixture proportions (Table 1) were designed to represent low, intermediate and high plasticity soils
227 with sodium activated bentonite (a representative of the smectite family) used as it affects both the
228 geotechnical and the electrical response of soils (Kibria, 2014). The maximum percentage of bentonite
229 was restricted to 5% not to produce BECs greater than 0.3 S/m, compromising the ability of TDR to
230 characterise the soil (Mojid et al., 2013). The index properties of the mixtures, tested in accordance
231 with BSI (1990a), are presented in Table 1 . The soils were named according to their plasticity as low
232 (CL), intermediate (CI) and high (CH) plasticity clay (BSI, 1990a). It is noted however that CI would be
233 classed as CL in accordance with ASTM D2487 (ASTM, 2017). The initial VWC of the soil mixtures
234 (determined from oven drying at 105°C) was found to increase with the plasticity of the soil: CL-44%,
235 CI-55% and CH-61%.

236 ***Pore fluid analysis***

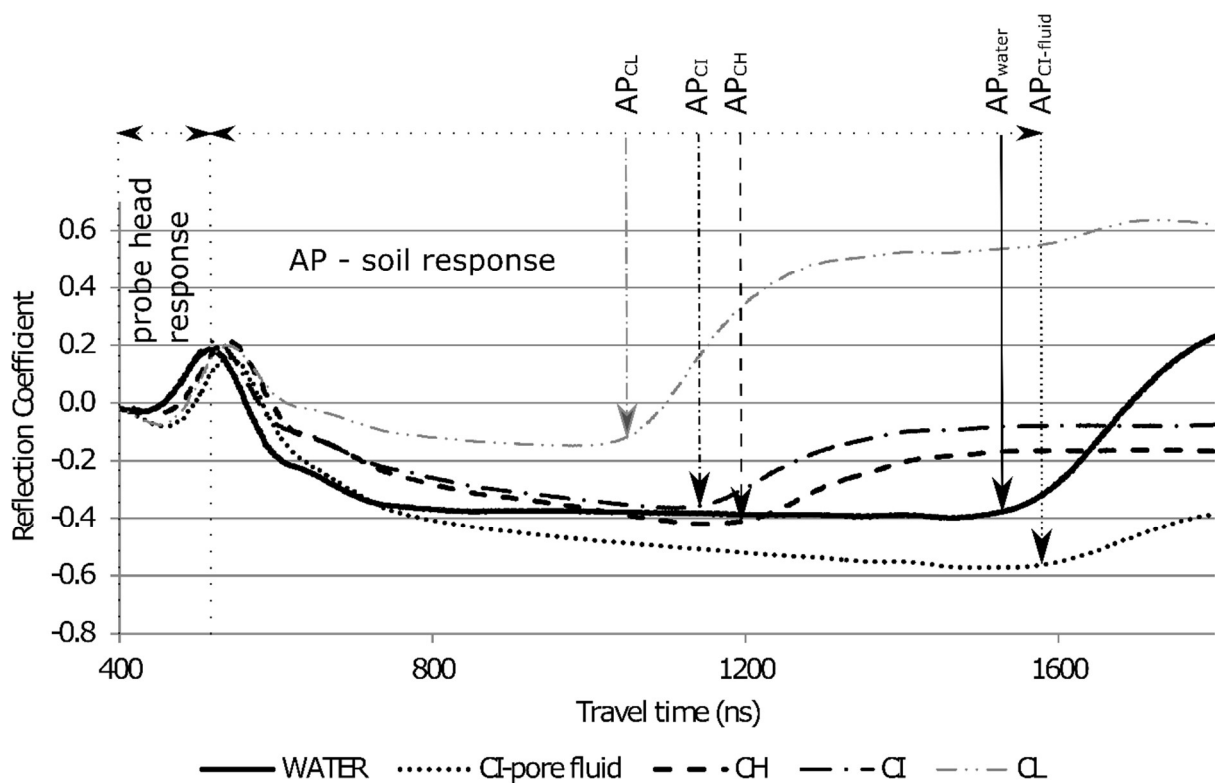
237 In order to investigate a chemical composition of the pore fluid that seeped out during the loading, an
238 inductively coupled plasma atomic emission spectroscopy (ICP-OES) analyses were conducted. Where
239 the pore volume was sufficient to immerse the TDR probe, its BEC was also compared with a low
240 frequency (11 Hz) electrical resistivity (ER) method. The ER measurements were conducted using
241 commercial soil boxes connected to an acquisition system (Faroqy, 2018). In order to differentiate
242 between the TDR and ER measured electrical conductivity, they are referred as BEC and EC
243 respectively.

244

245 **Results and Discussion**

246 **Initial TDR response prior to loading**

247 Initial TDR readings were taken prior to the application of loading for all the specimens. Examples of
 248 the measured waveforms are presented in Figure 4 for soils at their LL or slightly above, deionised
 249 water and for the pore fluid collected during the vertical loading of the CI soil.



250
 251 **Figure 4. TDR waveforms in deionised water (WATER); in the pore fluid from the CI soil (CI-pore**
 252 **fluid) and representative examples of the three soil mixtures prior to loading (CH; CI and CL). The**
 253 **vertical arrows indicate approximate apparent permittivity (AP) magnitude (Table 3) calculated on**
 254 **the basis of the form of the waveform’s travel time. Reflection coefficient amplitude translates to**
 255 **changes in the measured value of bulk electrical conductivity (BEC)**

256
 257 The waveforms shown in Figure 4 indicate that AP increased with the increase in the VWC and
 258 plasticity (Table 3), thus confirmed its relationship with VWC and LL in accordance with the literature
 259 (Topp et al., 1980, Thomas et al., 2010). Furthermore, higher signal attenuation due to increasing BEC
 260 was noted in those soil mixtures containing bentonite (as evidenced by the smaller magnitudes of the
 261 reflections). Despite significant differences in sand content between the CH (10% sand) and CI (50%

262 sand) soils mixtures, their initial AP and BEC were relatively close, Table 3. This was different than the
263 CL soil mixture (Table 3) and suggested a dominant influence of the bentonite on the TDR response.

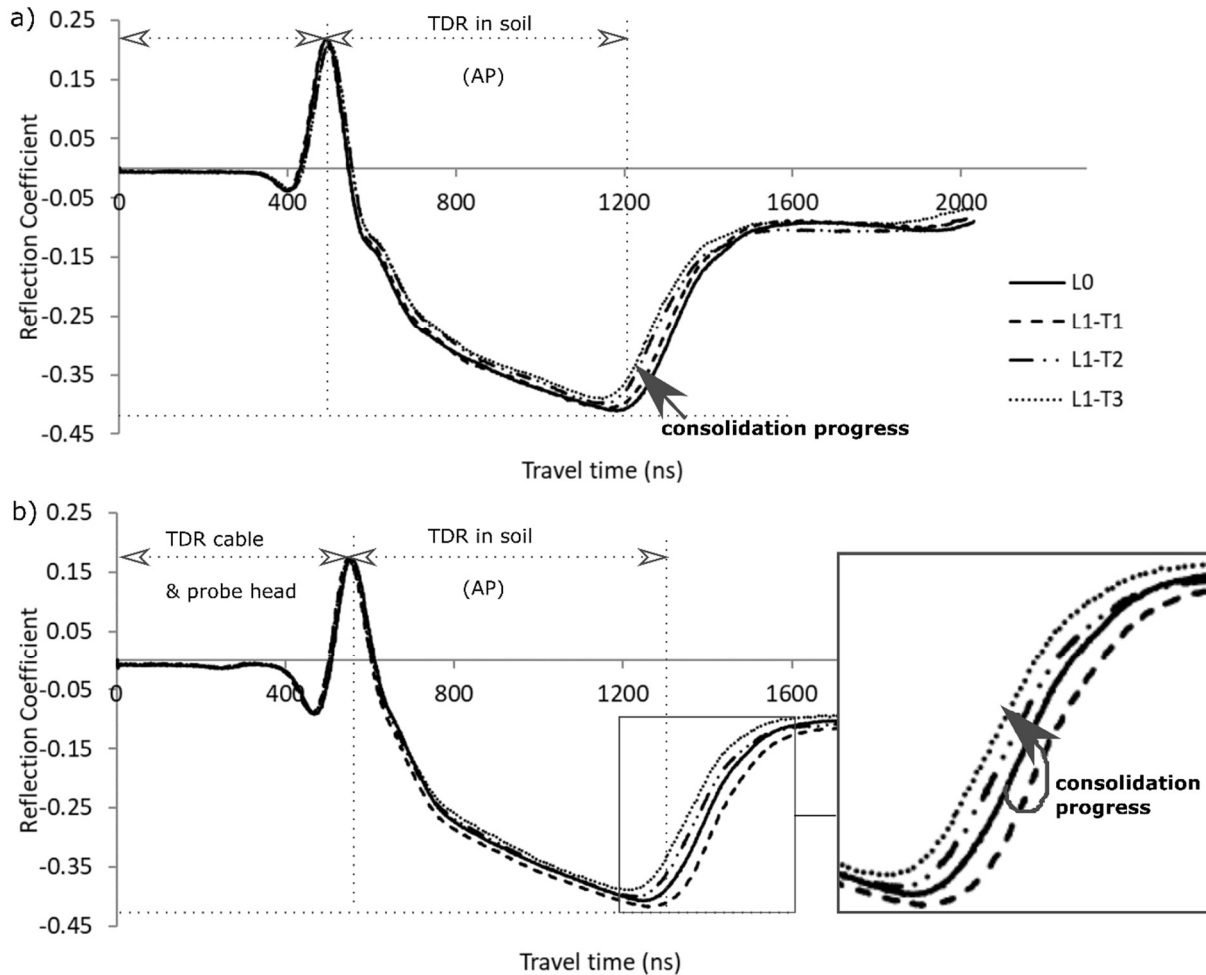
264 ***Variation of AP with loading in both vertical and horizontal orientations***

265 The reduction in the specimen height with load over time results from fluid expulsion and
266 consequential particle rearrangement (Barbour and Fredlund, 1989), which form the basis of the
267 compressibility estimation for each soil. Given that the electrical conduction in soils takes place
268 primarily through pore fluid electrolytes (Reynolds, 1997), it can be expected that the expulsion of
269 pore fluid containing solutes during consolidation results in a decreasing BEC. For example, a
270 correlation between e and EC during 1D consolidation has been found in sands (Comina et al., 2008),
271 and in clays with low, medium and high plasticity (McCarter and Desmazes, 1997; Fukue et al., 1999;
272 McCarter et al., 2005; Kibria, 2014) using low frequency ER measurements (0.01 Hz - 100 kHz).
273 Simultaneously, the decrease in the volume of water during consolidation is expected to change the
274 AP measured by TDR (Liu, 2007). This has been confirmed by the readings taken with the TDR_v probe,
275 showing that AP decreased with the expulsion of water following the application of the vertical load.
276 Figure 5a shows an example of the TDR_v waveforms obtained in a specimen of CI prior to the loading
277 (L0) and under the application of a 10 kPa load (L1) at three consecutive times (L1-T1, L1-T2, L1-T3),
278 corresponding to different consolidation stages presented on Figure 6 (T1 – 1 day, T2 – 14 days, T3 –
279 25 days after the load application). Whilst the start point does not change significantly with the
280 application of the load, the signal travel time (directly related to AP) noticeably reduces, resulting in
281 decreasing value of the measured AP. Therefore, if the soil is settling, vertical TDR measurements can
282 potentially detect this.

283 In contrast, the TDR_h readings for the same soil specimen (Figure 5b) did not follow the same trend
284 during the initial loading stages, showing an increase in travel time with drainage during the first
285 loading stage (L1-T1). Nonetheless, during the later stages of consolidation (L1-T2 and L1-T3) the travel

286 time reduced, resulting in a decrease in the measured AP. This response was observed also during
 287 further loading stages (L2 and L3), Figure 6.

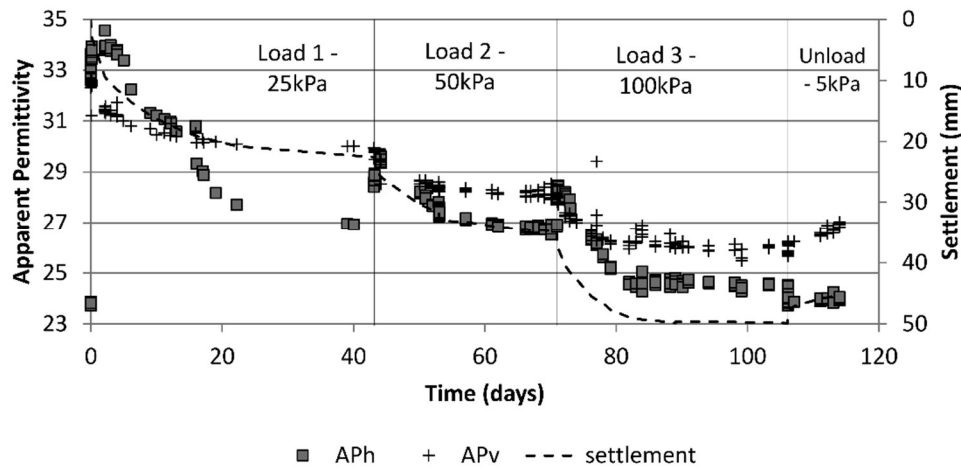
288



289

290 **Figure 5. a) TDR waveforms collected in the CI soil mixture from TDR_v prior to load application (L0)**
 291 **and at three consecutive points in time (T1-T3) following the application of a 10 kPa load (L1).**
 292 **Note the decrease in signal travel time response with increasing load and consolidation. b) TDR**
 293 **waveforms collected in the CI soil mixture from TDR_h at the same intervals as TDR_v. Note again the**
 294 **decrease in signal travel time response with increasing load and consolidation but only at times T2**
 295 **and T3.**

296 Based on Figure 5 AP has been calculated, which is presented in Figure 6 in relation to the settlement
 297 during the consolidation time. When the results, showed on Figure 6, are analysed in view of the AP
 298 change after each loading step in relation to the settlement, 1 unit of vertical AP change corresponds
 299 to approximately 7mm change in the sample height.



300

301 **Figure 6. AP determined from the vertical (AP_v) and horizontal TDR probe (AP_h) in response to**
 302 **changes in settlement in CI soil mixture. AP estimation error is within 0.1, whilst settlement –**
 303 **0.01mm**

304 If the vertically loaded soil was undergoing the same changes top and bottom of the specimen, then
 305 the relative change in measured parameters from TDR_h would be expected to be less than that of
 306 TDR_v . This is because a TDR probe provides a mean value for the AP encountered in a narrow volume
 307 along the electrode rods (Nissen et al., 2003; Pastuszka et al., 2014). In case of TDR_v , the probe
 308 averages the response of 75 mm thick soil layer, whilst TDR_h reflects approximately 10 mm in thickness
 309 above and below the probe's rods. Therefore, the relative change in AP (and GWC), for a localised
 310 region of the horizontal probe's rods is likely to be much less than along the length of vertical probe
 311 in these tests.

312 Two factors could explain the observed TDR_h responses: (i) a localised consolidation mechanism -
 313 increased density on the top of the TDR_h probe as a result of localised consolidation, even at the
 314 reduced load experienced at this depth; and/or (ii) seepage forces - the impact of densifying forces
 315 associated with the vertically downward seepage of pore water due to hydraulic gradient increase in
 316 the specimen.

317 *AP_h response: a localised consolidation mechanism*

318 With TDR_h lying in a horizontal plane, localised increase in density could exist around the probe's rods.
 319 TDR rod is a rigid intrusion in the soil and therefore, as the consolidation process takes place and the

320 soil moves past the rod, a void is created beneath that potentially fills with water (assuming that air
321 escaped as the loading process continued). The void would only fill with soil (collapse) if the shear
322 stress in the soil caused failure, which was unlikely to happen in this arrangement. This could not be
323 physically verified due to the very soft consistency of the specimens at the end of the tests.
324 Nonetheless, the visual observations during dissecting the specimen after the test indicated that the
325 soil 'shadowed' around the upper edge of the horizontal probe during consolidation, resulting in the
326 formation of a lower density 'pipe' underneath the rods. This 'pipe' is thought to have formed a
327 preferential fluid pathway towards the side of the chamber and hence drained pore waters from the
328 centre of the specimen. This localised volume would exhibit a higher water content compared to the
329 soil zones not affected by the presence of the probe. This hypothesis appeared to be confirmed by the
330 pore water pressure measurements (Figure 10) discussed further in the subsequent sections.

331 *AP_h response: Hydraulic gradient considerations*

332 Given that the chambers were 110 mm in internal diameter, and no grease was applied along the walls
333 due to the presence of the TDR instrumentation, the vertical load distribution through the specimen
334 was expected to be non-linear as the frictional forces between the consolidating specimen and
335 chamber wall increased with depth. As such, the upper layers of the specimen were likely to
336 experience a greater driver for consolidation than those lower down and the resultant flow pathways
337 from these upper layers would be shortest vertically upward. In specimens with very low hydraulic
338 conductivity, CH and CI, this resulted in accumulation of higher volume of water on the top than at
339 the bottom of the sample. Therefore, increasing hydraulic gradient (maximum 0.08 in CI) could
340 potentially impact on the consolidation process. However, it is considered to be too low, in
341 comparison with the vertical load imposed, to significantly affect the consolidation process.

342 **Relationship between AP and e**

343 Soil compressibility is often estimated based on C_c , derived from the $e - \log \sigma_v$ correlation. Therefore,
 344 correlation between TDR-derived AP and e could potentially enable further estimation of C_c . In all the
 345 experiments, e was derived from the specimen height (h), as shown in Equation 7.

$$e = (h - h_s)/h_s \tag{Equation 7}$$

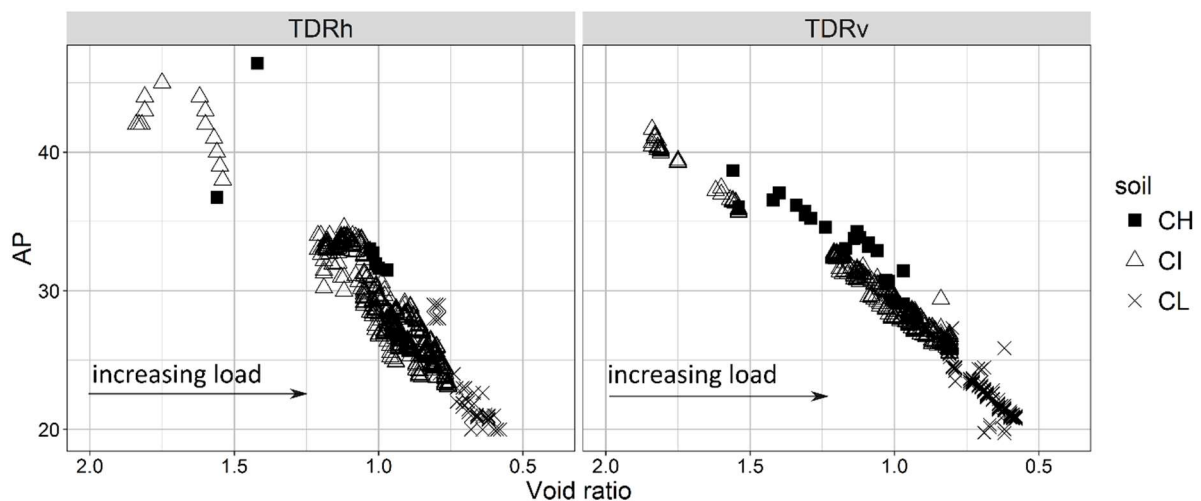
346 where h_s is the equivalent height of solids, as given by Equation 8.

$$h_s = h_0/(1 + e_0) \tag{Equation 8}$$

347 e_0 is an initial e , Equation 9, determined from GWC and G_s (the unit-less ratio of the unit weight of
 348 the solid particles to the unit weight of distilled water).

$$e_0 = GWC * G_s \tag{Equation 9}$$

349 A clear positive relationship between both vertical and horizontal measurements of AP and e was
 350 evident (Figure 7). This relationship is consistent with those previously reported in the literature for
 351 other materials (e.g., Liu, 2007; Jones and Friedman, 2000). The exact nature of the AP versus e
 352 relationship varied according to soil plasticity and water content of each specimen in the experiments
 353 and was affected by the TDR probe orientation. Whilst Jones and Friedman (2000), suggested nearly
 354 the same AP_v and AP_h values measured with TDR in glass bead mixtures, in the experiment conducted
 355 herein AP_v exhibited a stronger relationship with e , when compared to AP_h .



356

357 **Figure 7. TDR-derived apparent permittivity (AP) relationship compared to void ratio, e for all**
358 **three soil mixture during the vertical loading process (for all load steps AP measurements taken**
359 **with the probes orientated horizontally (TDR_h) and vertically (TDR_v)**

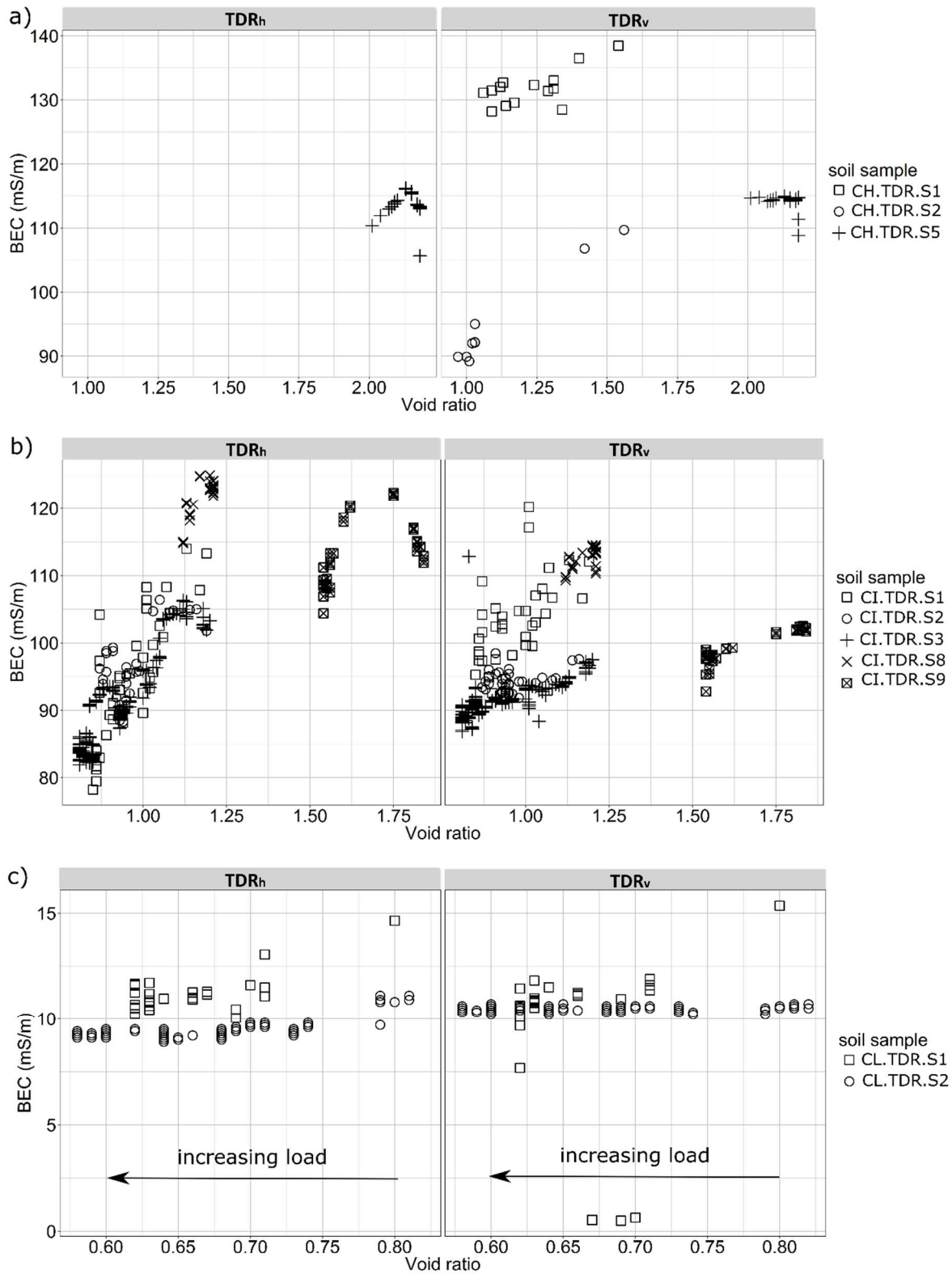
360

361 Given the factors described in the previous sections, the difference in the TDR_v and TDR_h response
362 with respect to e is considered a consequence of experimental set-up and localised impact of
363 consolidation. TDR_h was located in the bottom part of the specimen, where the acting load could be
364 approximately 20% lower than that experienced in the top layers, hence the change in the e calculated
365 for the whole specimen does not reflect the localised e changes in region of the TDR_h probe. It is clear,
366 however, that all tested soils followed the same overarching trend, i.e. decreasing AP with decreasing
367 e . Whilst the positive relationship between AP and e has been reported by other authors, based on
368 measurements taken at the end of consolidation experiments (Liu, 2007), this research showed that
369 the relationship can also be developed in real time during an active vertical loading process.
370 Furthermore, the findings of the current research indicate that although the settlement could be
371 potentially predicted based on the readings of either TDR_v or TDR_h, horizontally placed probed are
372 more affected by the initial pore water pressure increase.

373 ***Relationship between BEC and e***

374 Considering that the contribution of the electrolyte to BEC is restricted by the porosity of the medium
375 (Klein and Santamarina, 2003) and the influence of the conductive particles (Waxman and Smits,
376 1968), in saturated soils a gradual decrease in BEC would be expected with decreasing e . This general
377 decreasing trend can be seen in Figure 8, where the majority of the specimens show a ~10% drop in
378 BEC with increasing load and decreasing e . However, the CL samples and vertical response from
379 CH.S5.TDR did not display a clear trend. For CL specimens, Figure 8c, this could be attributed to the
380 significantly lower concentration of conductive ions and therefore the relative change in BEC is less
381 marked than in CI and CH specimens, Figure 8a. It is not obvious why the BEC response in CH.S5.TDR
382 was not sensitive to the void ratio changes. It is noted however that the specimen was prepared at 1.5

383 LL, hence its initial GWC was much higher than in two other CH specimens, prepared at 1.1 LL.
384 Potentially the conductivity of the solution did not change significantly for BEC to record the change.
385 Similar to the AP_h trends, shown in Figure 7, BEC_h appears to also respond to the increased influx of
386 water during initial loading. This is reflected in the 'parabolic' $BEC_h - e$ relationship that is particularly
387 pronounced in CI specimens and CH.TDR.S5, Figure 8b. This response is most likely affected by the
388 increased concentration of ions available around the horizontal TDR probe. Friedman (2005) suggests
389 that BEC is more sensitive to the pore connectivity than volume changes, which could explain why AP
390 (sensitive to the volumetric changes) correlates better with e than BEC.
391 The differences between BEC_v and BEC_h response was considered to be a result of discrepancies in the
392 density and compression of the specimens between the upper region (TDR_v) and lower (TDR_h), where
393 the probes sit.



394

395 **Figure 8. BEC versus void ratio for a) CH, b) CI and c) CL during consolidation with measurements**
 396 **taken using both TDR_v and TDR_h**

397

398 Given that pore fluid conductivity is the main medium conducting the current in saturated soils (Klein
399 and Santamarina, 2003), contribution of the pore fluid's electrical conductivity (EC_f) to the BEC of the
400 soil specimen was investigated. The EC_f measurements of the fluid, which seeped out after the loading,
401 were performed using the ER method (Faroqy, 2018). This approach enabled testing small volumes of
402 fluid available (7 ml) whilst it was possible to use the remaining fluid for the ICP-OES analyses. Where
403 the pore volume was sufficient to immerse the TDR probe, its BEC was compared with the ER method.
404 The results indicated that the two techniques produced similar results, as the BEC of the pore fluid
405 measured with TDR corresponded to approximately 0.288 S/m; whilst the EC_f measured with the ER
406 was at 0.275 S/m in CI specimens.

407 The EC_f results (Table 4) confirmed that smectites had a dominant influence on the salt content of the
408 pore fluid due to the much higher availability of exchangeable ions when compared to kaolinite. This
409 was confirmed by the ICP-OES chemical results showing sodium as a dominant component in the pore
410 fluid from sodium activated soil (Table 5) and a close EC_f range for CH and CI with values of 0.247 S/m
411 and 0.275 S/m respectively (Table 4). Due to its high mobility, Na was found to have a significant
412 impact on EC_f (Rinaldi and Cuestas, 2002). In contrast, CL, which contained sand and kaolinite, had an
413 EC_f seven times smaller (approximately 0.041 S/m). Given that the BEC of soil is dominated by BEC
414 (Cassidy, 2009; Jung et al., 2013a), BEC can be seen as an indicator of a degree to which solid particles
415 constrain the electromagnetic response of free fluid: the BEC of the CH specimens (with 10% sand)
416 was 50% of the EC_f value and 25% in the CI specimens (with 50% sand). In the CL soil (with 50% sand),
417 containing no bentonite, the sand effect was even more predominant, resulting in the soil BEC being
418 25% of its EC_f . Following from this, the BEC/ EC_f (Table 1) relationship (expressed as a percentage)
419 reflects the LL of the samples (Table 4).

420 Rosenbourn (1976) observed that the concentration of conductive ions in the pore fluid of soils
421 containing montmorillonite decreased with the increasing effective stress during consolidation. In the
422 present study, the EC_f and the chemical composition of the combined fluid were found to be very
423 similar in several CI specimens (Table 2 and Table 5). This however, does not provide an answer to

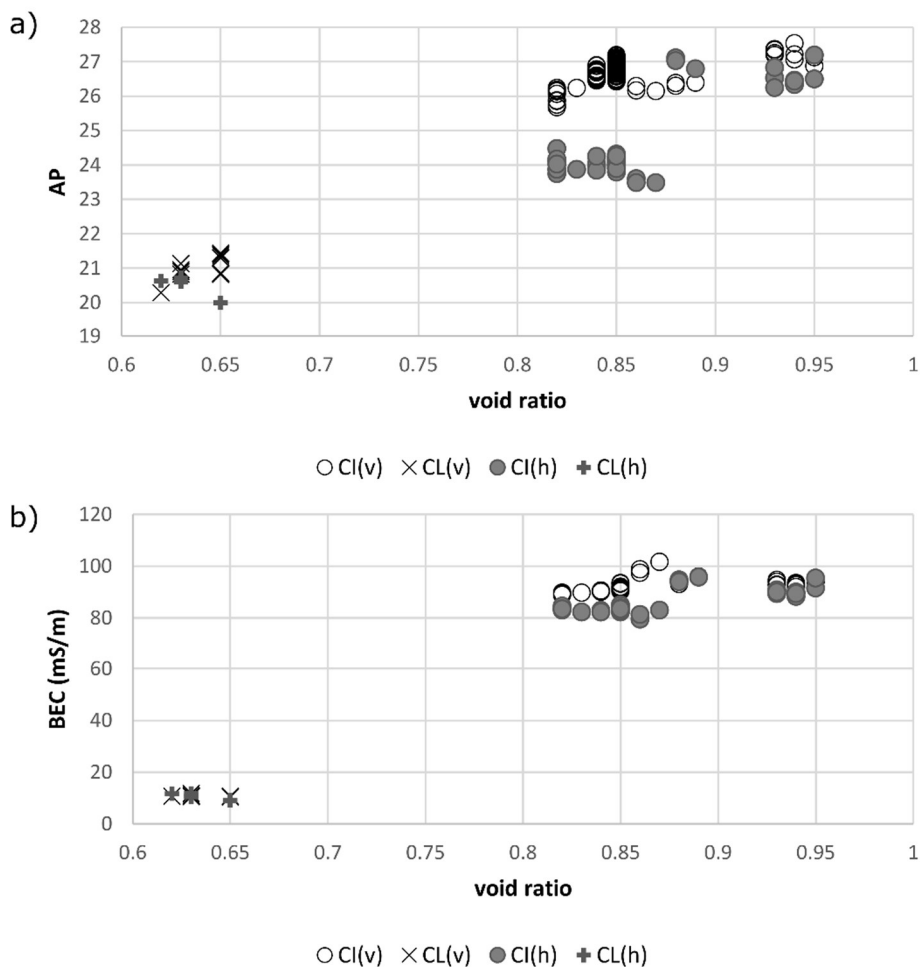
424 whether the EC_f was changing during consolidation. The response of BEC and EC in soils containing
425 bentonite remains an active area of research. Using low frequency ER measurements, Fukue (1999)
426 found that the EC of soils containing bentonite started increasing at loading stages exceeding 78 kPa,
427 which was hypothesised to result from the diffusive double layer (DDL) deformation. Similarly, an
428 increase in the value of BEC in a soil containing 60% montmorillonite was observed using TDR when
429 the applied pressure exceeded 110 kPa (Liu, 2007). The latter was attributed to pore fluid salinity
430 dependent DDL suppression, which was hypothesised (Liu, 2007) to increase BEC with a decrease in
431 VWC in soils with a BEC of pore fluid below 0.2 S/m, however there was no experimental proof
432 supporting this theory. The suppression of is expected with an increase in ion concentration in the
433 pore fluid (Sridharan, 1982) and given that the long range electrical repulsive forces (DDL) resist the
434 compression at a given external applied pressure in smectite containing soils (Sridharan and Rao,
435 1973), information about EC_f within the soil pores could provide further insight into the soil response
436 to loading and unloading. Currently, TDR readings provide only a bulk response, reflecting closing of
437 the pore spaces during loading and possible changes in the pore fluid. However, it is apparent that
438 pore-scale changes in a soil specimen, which will result in changes in geotechnical properties, can be
439 detected using TDR methods. This is clearly an important, and potentially far reaching finding as it
440 provides a proxy monitoring/evaluation tool for such processes.

441 ***TDR response to unloading***

442 During unloading, the physical and chemical bonds between the particles that are developed during
443 the loading process break apart (Terzaghi et al., 1996). Negative porewater pressure is generated and
444 the excess pore water pressures lead to the heave of the specimens as water is drawn back into the
445 soil.

446 In kaolinite soils, the rebound (heave) is controlled only by the hydrostatic pressure deficiency
447 developed in the undrained phase; whereas in smectite dominated soils, also DDL repulsive forces
448 affect its magnitude (Sridharan and Rao, 1973). In the soils considered herein (where the bentonite

449 content was limited to 5% by weight of the specimen) it is suspected that both mechanisms will be
 450 prevalent in the CI and CH specimens. Testing of the electrical response to unloading was limited to
 451 five specimens (including only CL and C soils) and a maximum of two unloading steps; nonetheless, it
 452 was interesting to note that when unloaded both AP and BEC measured in both directions rebounded
 453 in several samples as water was drawn back into the soil fabric (Figure). Although, the unloading was
 454 very limited and the magnitude of load removed differed across the samples (Table 2), it appeared
 455 that AP and BEC changes can be observed when a sufficient load is removed (unloading in small
 456 graduations did not result in observable changes). Given that the rebound was limited by the swelling
 457 properties of the CH, CI and CL soils as indicated by the C_s values of 0.08, 0.05 and 0.03 respectively,
 458 the volumes of water being drawn into the specimen are relatively small. Nonetheless, it was
 459 encouraging to observe that even these small changes can be reflected in the AP and BEC readings.



460

461 **Figure 9. Relationship between void ratio, e and a) apparent permittivity (AP), b) bulk electric**
462 **conductivity (BEC) measured in the direction of the load application (v) and normal to the load**
463 **application (h) during unloading of three CI (CI.S01, CI.S02, CI.S3.TDR) and two CL specimens**
464 **(CL.S1.TDR, CL.S2.TDR); no unloading was carried out on the CH samples**

465

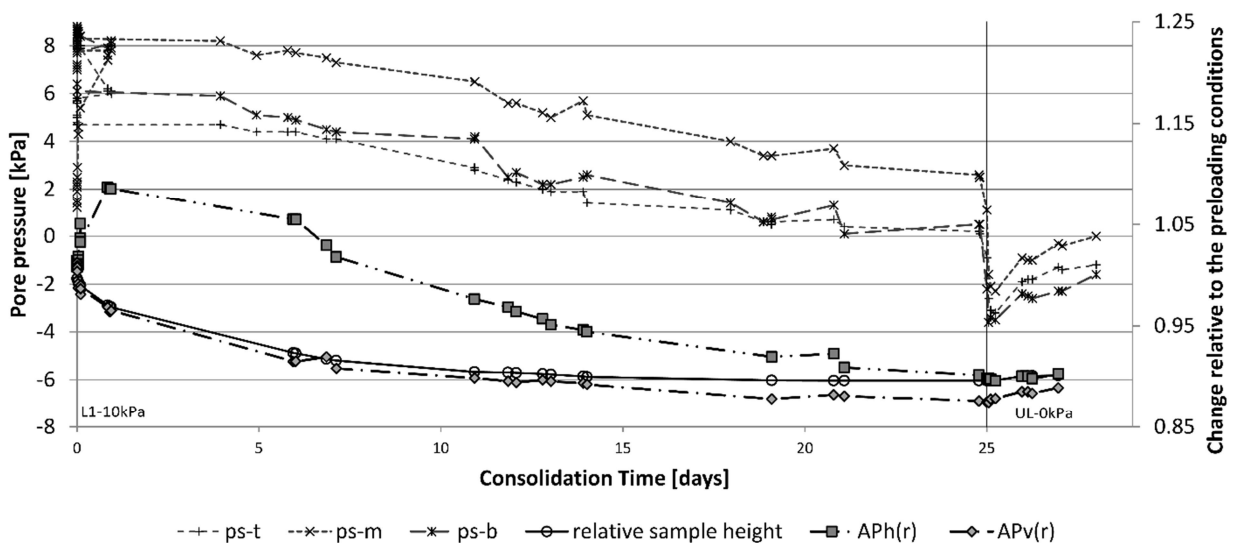
466 It is suggested that there is a sensitivity threshold, which is either a function of the experimental
467 apparatus used herein, or a function of the change in void space within the soil (and the concentration
468 of ions being drawn back into the soil), or both. It is noted that, although this rebound was observed
469 in a laboratory setting, in field conditions the magnitude of change may lie within the sensitivity
470 limitations of the equipment and requires further research.

471 *TDR response to pore water pressure changes*

472 The AP_h was noted to increase immediately after the load was applied, whilst AP_v was decreasing with
473 the progress of settlement. In order to investigate this relationship further, pore water pressure
474 response was monitored on selected samples. The consolidation chamber was instrumented with the
475 external pore water pressure sensors positioned at three depths: height of TDR_v (ps-t), in the middle
476 of the specimen (ps-m) and at the same height as TDR_h (ps-b), Figure 2. The change in the AP_v and AP_h
477 was plotted as relative terms against consolidation time ($AP_{v(r)}$ and $AP_{h(r)}$ respectively) with the
478 absolute values normalised to the initial values - Figure 10, indicating that the rate of the AP_h increase
479 corresponded with that of the bottom pore water pressure response (ps-b) located at the same depth
480 as the TDR_h . The $AP_{h(r)}$ was consistently greater than $AP_{v(r)}$, suggesting a region of higher water content
481 near the horizontal probe. The time lag between the commencement of the settlement of the soil
482 specimens and the decrease in the AP_h appears proportional to the plasticity and, as such, the
483 compressibility of the soil (C_c of CH, CI and CL was in the order of 0.38, 0.32, 0.13 respectively). This
484 effect was initially thought to be a result of the pore water pressure changes in the specimen due to
485 the consolidation pressure. However, the additional tests in pressurised chambers (Faroqy, 2018)
486 indicate that neither AP nor BEC responded to the pressure increase. As such, it is most likely
487 influenced by physical changes in the soil as a response to the increased pressure. Primarily, the

488 consolidation mechanism, which principally affected the upper layers of the soil due to the non-linear
 489 load distribution within the soil specimen, resulted in the densification of the upper layers of soil much
 490 earlier than deeper layers. Meanwhile, the emplacement of the TDR rods horizontally into the soil
 491 resulted in a small 'load-shadow' being developed directly under the rods which created a softer zone
 492 of soil below them. This may have provided a preferential pathway for water to seep out of the soil
 493 mass from the centre of the specimen, along the softer zone around the TDR rods and then down the
 494 chamber-soil interface. Given that TDR measurements are related to water content, it is believed that
 495 the initial increase in TDR_h readings seen in CH and CI, reflects the changes induced by pore water
 496 pressure with loading. This effect was not observed in CL as the pore pressure dissipated very quickly
 497 due to the higher hydraulic conductivity. Interestingly, the time at which the relative values of AP_h
 498 and AP_v begin to merge correspond with the end of the primary consolidation time, which could be
 499 used as a very useful tool to monitor the progress of consolidation.

500 The $AP_{v(r)}$ and $AP_{h(r)}$ results suggest that the consideration of the load direction during instrumentation
 501 of a specimen/site is of significant importance. In circumstances when a soil is subject to loading in
 502 saturated (or near-saturated) conditions, the probes normal to the loading direction (here TDR_h)
 503 appear to be responsive to the pore water pressure induced changes; whilst probes positioned parallel
 504 (TDR_v) respond to structural changes.



505

506 **Figure 10. Relative AP_h and AP_v changes (normalised by the pre-loading measurement) in relation**
507 **to the settlement and the pore pressure dissipation recorded at the top ($ps-t$), in the middle ($ps-m$)**
508 **and at the height of the TDR_h ($ps-b$). L = loading phase, UL = unloading phase.**

509

510 **Conclusions and Recommendations**

511 Regular monitoring of the AP and BEC response to the changes in saturated, fine-grained soils under
512 vertical loading in the controlled laboratory conditions indicated a positive and clear relationship
513 between the AP response, measured in the direction of the load application (vertically), and void ratio
514 of soils with a range of plasticity. Changes in the geotechnical parameters were measured in terms of
515 the bulk parameters derived from the initial and final GWC and sample-height measurements during
516 loading and unloading. Measurements taken in two perpendicular directions allowed further insights
517 to be gained on the initial response of the soil to the application of a load. Whilst the AP measured
518 vertically decreased gradually with loading, horizontal probes exhibited elevated AP levels during
519 initial loading stages and gradually decreased with the progress of consolidation. AP_v was found to
520 correlate very well with e , whilst AP_h coincided with the increased pore water pressure dissipation. It
521 is thought that the load application forced ingress of water locally around the horizontal probe due to
522 excess pore water pressure in this experimental setup. Nonetheless, the same conditions are likely to
523 take place on site. Given that the magnitude of the relative change in AP_v and AP_h began to merge at
524 the time relating to the end of the primary consolidation stage, it is possible that this observation
525 could be used to monitor the progress of consolidation *in-situ* before the ground movement damage
526 is inflicted on the ground surface. Simultaneously, BEC values exhibited a tendency to mirror the AP
527 response; however, more scatter in the results was observed. BEC was found to be correlated with e
528 in a few samples; however, there were also cases where it plateaued whilst the structural changes
529 continued to take place. This suggests that pore connectivity rather than the void ratio has a
530 predominant effect on the values of BEC. Correlation of BEC with the pore fluid conductivity revealed

531 very close relationship with LL, which could potentially be used as LL indicator depending on the soil
532 conditions.

533 Most interestingly, the two-directional positioning of the TDR probes can provide insights into the
534 spatial and temporal changes in soils during settlement. Whilst AP_v can indicate decreasing e (or VWC)
535 with loading, the initially elevated AP_h response can indicate pore water pressure dissipation. This is a
536 unique and novel finding, encouraging for the monitoring of saturated earthwork structures under
537 cyclic loads. Simultaneously, this finding has an implication on the application of TDR in VWC
538 measurements. TDR measured VWC will be overestimated if it is obtained from a probe embedded
539 horizontally in a soil subject to vertical loading.

540 The unloading process was monitored with TDR for the first time. Although this aspect was
541 investigated on a limited scale, both BEC and AP readings increased slightly with the increase in void
542 ratio. This indicated potential applicability of TDR in monitoring the progress of unload.

543 Due to the observed AP_v correlation with e , AP_h correlation with the pore water induced changes, and
544 the relationship between AP_v and AP_h , it is the authors' contention that regular, near surface-based
545 monitoring, using TDR could be very informative for *in-situ* settlement monitoring. Relative changes
546 could be used to inform of the comparative 'health' of the asset, with trigger levels designated when
547 corrective action may be required. Monitoring such relative changes in AP (or similar) over time would
548 extend our understanding of how soils respond to changes in physical conditions (environment,
549 loading, etc.). Trigger levels for the geophysical parameters could be set where, if exceeded, additional
550 investigations could be carried out to assess the relative stability of the asset in more detail.

551 **Data Availability**

552 Some or all data, models, or code generated or used during the study are available from the
553 corresponding author by request.

554 **Acknowledgements**

555 The authors greatly acknowledge the UK's Engineering and Physical Sciences Research Council
556 (EPSRC) and the "Assessing The Underworld" (ATU) project (grant No. EP/KP021699/1) for the
557 financial support provided and the University of Birmingham for the access to the testing materials
558 and facilities. Special thanks go to the technicians of the Civil Engineering laboratories who built the
559 testing setup.

560

561 **References**

- 562 Abu-Hassanein, Z.S., Benson, C.H. and Blotz, L.R. (1996) Electrical resistivity of compacted clays.
563 **Journal of Geotechnical Engineering**, 122 (MAY): 397–406.
- 564 ASTM D2487-17 (2017) Standard Practice for Classification of Soils for Engineering Purposes (Unified
565 Soil Classification System), ASTM International, West Conshohocken, PA.
- 566 Barbour, S.L. and Fredlund, D.G. (1989) Mechanisms of osmotic flow and volume change in clay soils.
567 **Canadian Geotechnical Journal**, 26 (4): 551–562.
- 568 Basu, D., Misra, A., Puppala, A.J., et al. (2013) Sustainability in geotechnical engineering – general
569 report. **Proceedings of the 18th ICSMGE, Paris** [online], 7062 (ii): 3155–3162.
- 570 BSI (1990a) "Part 2: Classification tests. BS 1377-2: 1990." In *Methods of test for soils for civil*
571 *engineering purposes*. London.
- 572 BSI (1990b) "Part 6: Consolidation and permeability tests in hydraulic cells and with pore pressure
573 measurement. BS 1377-6: 1990." In *Methods of test for soils for civil engineering purposes*. London.
- 574 Cassidy, N.J. (2009) "ELECTRICAL AND MAGNETIC PROPERTIES OF ROCKS , SOILS AND FLUIDS." In Jol,
575 H.M. (ed.) **Ground Penetrating Radar: Theory and Applications**. First Edit. Amsterdam: Elsevier. pp.
576 41–72.
- 577 Charles, J. A., Tedd, P., Warren, A. (2011) Lessons Learnt from Dam Incidents. Report SC080046/R1.
578 Environment Agency, Bristol.
- 579 Clarke, B.G., Middleton, C. and Rogers, C. (2016) The Future of Geotechnical and Structural
580 Engineering Research. **Proceedings of the Institution of Civil Engineers - Civil Engineering**, 169 (1).
- 581 Comina, C., Foti, S., Musso, G., et al. (2008) EIT oedometer: An advanced chamber to monitor spatial
582 and time variability in soil with electrical and seismic measurements. **Geotechnical Testing Journal**,
583 31 (5): 404–412.
- 584 Curioni, G., Chapman, D.N., Metje, N., et al. (2012) Construction and calibration of a field TDR
585 monitoring station. **Near Surface Geophysics**, 10 (3): 249–261.

586 Curioni, G., Chapman, D.N., Pring, L.J., et al. (2018a) Extending TDR capability for measuring soil
587 density and water content for field condition monitoring. **Journal of Geotechnical and**
588 **Geoenvironmental Engineering**, 144 (2).

589 Curioni, G., Chapman, D.N., Royal, A.C.D., Metje, N., Dashwood, B., Gunn, D.A., Inauen, C.M.,
590 Chambers, J.E., Meldrum, P.I., Wilkinson, P.B., Swift, R.T., Reeves, H.J., (2018b). TDR potential for soil
591 condition monitoring of geotechnical assets. **Canadian Geotechnical Journal** (accepted).

592 Ekblad, J. and Isacsson, U. (2007) Time-domain reflectometry measurements and soil-water
593 characteristic curves of coarse granular materials used in road pavements. **Canadian Geotechnical**
594 **Journal**, 44: 858–872.

595 Farooq, A. (2018) ‘Investigating the Changes in the Geophysical and Geotechnical Properties of Fine-
596 grained Soils when Exposed to Changes in Vertically Applied Loads’, PhD thesis, University of
597 Birmingham.

598 Friedman, S.P. (2005) Soil properties influencing apparent electrical conductivity: A review.
599 **Computers and Electronics in Agriculture**.

600 Fukue, M., Minato, T., Horibe, H., et al. (1999) The micro-structures of clay given by resistivity
601 measurements. **Engineering Geology** [online], 54 (1–2): 43–53.

602 Heimovaara T.J. and Bouten W. (1990) A Computer-Controlled 36-Channel Time Domain
603 Reflectometry System for Monitoring Soil Water Contents. **Water Resources Research**, 26 (10):
604 2311-2316.

605 Huisman, J. a., Lin, C.P., Weihermüller, L., et al. (2008) Accuracy of Bulk Electrical Conductivity
606 Measurements with Time Domain Reflectometry. **Vadose Zone Journal**, 7 (2): 426–433.

607 Janik, G., Dawid, M., Walczak, A., et al. (2017) Application of the TDR technique for the detection of
608 changes in the internal structure of an earthen flood levee. **Journal of Geophysics and Engineering**,
609 14: 292–302.

610 Jones, S.B. and Friedman, S.P. (2000) Particle shape effects on the effective permittivity of
611 anisotropic or isotropic media consisting of aligned or randomly oriented ellipsoidal particles. **Water**
612 **Resources Research** [online], 36 (10): 2821–2833.

613 Jones, S.B., Wraith, J.M. and Or, D. (2002) Time domain reflectometry measurement principles and
614 applications. **Hydrological Processes** [online], 16 (1): 141–153.

615 Jung, S., Drnevich, V. P., and Abou Najm, M. R. (2013a). “New methodology for density and water
616 content by time domain reflectometry.” **Journal of Geotechnical and Geoenvironmental**
617 **Engineering**, 139 (5), 659–670.

618 Jung, S., Drnevich, V. P., and Abou Najm, M. R. (2013b). “Temperature corrections for time domain
619 reflectometry parameters.” **Journal of Geotechnical and Geoenvironmental Engineering**, 139(5):
620 671-683.

621 Keller, G. and Frischknecht, F.C. (1966) “Electrical methods in geophysical prospecting.” **In Volume**
622 **10 of International series of monographs on electromagnetic waves**. Pergamon Press.

623 Kibria, G. (2014) **Evaluation of Physico-Mechanical Properties of Clayey Soils Using Electrical**
624 **Resistivity Imaging Technique**, PhD thesis, University of of Texas at Arlington.

- 625 Klein, K.A. and Santamarina, J.C. (2003) **Electrical Conductivity in Soils : Underlying Phenomena.**
626 *Journal of Environmental and Engineering Geophysics*, December 2003, Volume 8, Issue 4, pp. 000–
627 000.
- 628 Lambot, S., Grandjean, Samyn, K., Cousin, I., Thiesson, J., Stevens, A., Chiarantini, L., Dahlin, T. (2009)
629 **Technical specifications of the system of geophysical sensors.** Report N° FP7-DIGISOILD1.1, 86
630 pages.
- 631 Liu, N. (2007) **Soil and site characterization using electromagnetic waves** [online]. Virginia
632 Polytechnic Institute and State University.
- 633 McCarter, W.J., Blewett, J., Chrisp, T.M., et al. (2005) Electrical property measurements using a
634 modified hydraulic oedometer. **Canadian Geotechnical Journal**, 42: 655–662.
- 635 McCarter, W.J. and Desmazes, P. (1997) Soil characterization using electrical measurements.
636 **Geotechnique**, 47 (1): 179–183.
- 637 McDowell, P., Barker, R., Butcher, A., et al. (2002) Geophysics in engineering investigations.
638 **Geological Society, London, Engineering Geology Special Publications** [online], p. 260.
- 639 Mitchell, J. and Liu, N. (2006) Usefulness of EM waves for site and soil property characterization in
640 geotechnical engineering. **ASCE Geotechnical Special Publication**, (Gsp 149): 136–143.
- 641 Mitchell, J. and Soga, K. (2005) **Fundamentals of soil behavior**. Third. Hoboken: John Wiley and Sons,
642 Inc.
- 643 Mojid, M.A., Wyseure, G.C.L. and Rose, D.A. (2003) Electrical conductivity problems associated with
644 time-domain reflectometry (TDR) measurement in geotechnical engineering. **Geotechnical and**
645 **Geological Engineering**.
- 646 Nissen, H.H., Ferré, T.P.A. and Moldrup, P. (2003) Sample area of two- and three-rod time domain
647 reflectometry probes. **Water Resources Research**, 39 (10): 1–11.
- 648 Olson, R.E. (1986) “State of the art: consolidation testing.” In Yong R. N. and C., T.F. (eds.)
649 *Consolidation of soils: testing and evaluation. Special technical publication STP 892.* West
650 Conshohocken, PA: American Society for Testing and Materials. pp. 7–70.
- 651 Pastuszka, T., Krzyszcak, J., Sławiński, C., et al. (2014) Effect of Time-Domain Reflectometry probe
652 location on soil moisture measurement during wetting and drying processes. **Measurement: Journal**
653 **of the International Measurement Confederation**, 49: 182–186.
- 654 Reynolds, J.M. (1997) **An Introduction to Applied and Environmental Geophysics.**
- 655 Rosenbaum, M.S. (1976) Effect of Compaction on the Pore Fluid Chemistry of Montmorillonite. *Clays*
656 *and Clay Minerals*, 24: 118–121.
- 657 Rinaldi, V. a. and Cuestas, G. a. (2002) Ohmic Conductivity of a Compacted Silty Clay. **Journal of**
658 **Geotechnical and Geoenvironmental Engineering**, 128 (October): 824–835.
- 659 Robinson, D.A., Jones, S.B., Wraith, J.M., et al. (2003) A review of advances in dielectric and electrical
660 conductivity measurement in soils using time domain reflectometry. **Vadose Zone Journal**, 2 (4):
661 444–475.
- 662 Rogers, C.D.F., Hao, T., Costello, S.B., et al. (2012) Condition assessment of the surface and buried
663 infrastructure - A proposal for integration. **Tunnelling and Underground Space Technology**, 28 (1):

664 202–211.

665 Rosenbaum, M.S. (1976) Effect of Compaction on The Pore Fluid Chemistry of Montmorillonite. *Clays*
666 *and Clay Minerals*, 24: 118–121.

667 Royal, A.C.D., Atkins, P.R., Brennan, M.J., et al. (2011) Site Assessment of Multiple-Sensor
668 Approaches for Buried Utility Detection. **International Journal of Geophysics** [online], 2011: 1–19.

669 Sadeghioon, A., Metje, N., Chapman, D., et al. (2014) SmartPipes: Smart Wireless Sensor Networks
670 for Leak Detection in Water Pipelines. **Journal of Sensor and Actuator Networks** [online], 3 (1): 64–
671 78.

672 Schon, J.H. (2004) *Physical properties of rocks: fundamentals and principles in petrophysics*. Oxford:
673 Elsevier.

674 Shah, J., Jefferson, I. and Hunt, D. (2014) Resilience assessment for geotechnical infrastructure
675 assets. *Infrastructure Asset Management*, 1 (4): 95–104.

676 Skierucha, W., Wilczek, a. and Walczak, R.T. (2004) Polowy system monitorowania parametrów
677 fizykochemicznych gleb i gruntów. **Acta Agrophysica**, 4 (2): 533–545.

678 Sridharan, A. and Rao, G.V. (1973) Mechanisms controlling volume change of saturated clays and the
679 role of the effective stress concept. *Géotechnique*, 23 (3): 359–382.

680 Sridharan, A. and Jayadeva, M.S. (1982) Double layer theory and compressibility of clays.
681 *Geotechnique*, 32 (2): 133–144.

682 Terzaghi, K., Peck, R.B. and Mesri, G. (1996) **Soil Mechanics in Engineering Practice Third Edition**.
683 John Wiley & Sons.

684 Thring, L.M., Boddice, D., Metje, N., et al. (2014) Factors affecting soil permittivity and proposals to
685 obtain gravimetric water content from time domain reflectometry measurements. *Canadian*
686 *Geotechnical Journal*, 51 (11): 1303–1317.

687 Thomas, A.M., Chapman, D.N., Rogers, C.D.F., et al. (2010) Electromagnetic properties of the ground:
688 Part I – Fine-grained soils at the Liquid Limit. **Tunnelling and Underground Space Technology**
689 [online], 25 (6): 714–722.

690 Topp, C., Resource, L. and Canada, A. (1980) **Electromagnetic Determination of Soil Water Content**,
691 16 (3): 574–582.

692 Thring, L.M., Boddice, D., Metje, N., et al. (2014) Factors affecting soil permittivity and proposals to
693 obtain gravimetric water content from time domain reflectometry measurements. *Canadian*
694 *Geotechnical Journal*, 51 (11): 1303–1317.

695 Waxman, M.H. and Smits, L.J.M. (1968) Electrical Conductivities in Oil-Bearing Shaly Sands. **Society**
696 **of Petroleum Engineers Journal**. 8

697

698 **List of Symbols**

Symbol	Unit	Description
AP	-	Apparent Permittivity
AP _h	-	AP measured with TDR _h
AP _v	-	AP measured with TDR _v
AP _(r)	-	AP normalised by an initial reading
BEC	S/m	Bulk Electrical Conductivity (measured with TDR)
BEC _h	S/m	BEC measured with TDR _h
BEC _v	S/m	BEC measured with TDR _v
C _c	-	Compression index
CH	-	High plasticity clay
CI	-	Intermediate plasticity clay
CL	-	Low plasticity clay
C _s	-	Swelling index
DDL	-	Diffusive double layer
e	-	Void ratio
EC _{dc}	S/m	Direct current electrical conductivity
EC _f	S/m	EC of pore fluid measured with ER method
ER	-	Electrical Resistivity method (11Hz)
G _s	Mg/m ³	particle density
GWC	g/g	Gravimetric water content
h	m	specimen height

ICP-	-	inductively coupled plasma optical emission spectrometry
OES		
LL	%	Liquid Limit
m_s	g	Dry mass of soil (after oven drying in 105 °C)
m_v	m^2/kN	Coefficient of volume compressibility
PI	%	Plasticity Index (PI=LL-PL)
PL	%	Plastic Limit
TDR	-	Time Domain Reflectometry
TDR _h	-	TDR probe positioned normally to the direction of loading (horizontal plane)
TDR _v	-	TDR probe positioned in the direction of loading (vertical plane)
V	m^3	volume
VWC	%	Volumetric water content
ρ_d	Mg/m^3	Dry density
σ_v	kPa	Effective stress in the vertical direction

699 Figure captions

700 Figure 1. TDR chamber set-up under load conditions: 1 - compression gauge, 2- vertical TDR probe, 3
701 - horizontal TDR probe, 4 - loading frame, 5 - bottom drainage pipe, 6 - drainage container.
702 Figure 2. Schematic of the TDR chamber equipped with the pore pressure sensors (PS), positioned at
703 the bottom (b), middle (m) and top (t) of the chamber, measurements in mm
704 Figure 3. TDR measurements taken in DI water in the chamber and larger bucket to investigate the
705 container effect on the measurements
706 Figure 4. TDR waveforms in deionised water (WATER); in the pore fluid from the CI soil (CI-pore fluid)
707 and representative examples of the three soil mixtures prior to loading (CH; CI and CL). The vertical
708 arrows indicate approximate apparent permittivity (AP) magnitude (Table 3) calculated on the basis
709 of the form of the waveform's travel time. Reflection coefficient amplitude translates to changes in
710 the measured value of bulk electrical conductivity (BEC)
711 Figure 5. a) TDR waveforms collected in the CI soil mixture from TDR_v prior to load application (L0)
712 and at three consecutive points in time (T1-T3) following the application of a 10 kPa load (L1). Note
713 the decrease in signal travel time response with increasing load and consolidation. b) TDR
714 waveforms collected in the CI soil mixture from TDR_h at the same intervals as TDR_v. Note again the

715 decrease in signal travel time response with increasing load and consolidation but only at times T2
716 and T3.
717 Figure 6. AP determined from the vertical (AP_v) and horizontal TDR probe (AP_h) in response to
718 changes in settlement in CI soil mixture. AP estimation error is within 0.1, whilst settlement –
719 0.01mm
720 Figure 7. TDR-derived apparent permittivity (AP) relationship compared to void ratio, e for all three
721 soil mixture during the vertical loading process (for all load steps AP measurements taken with the
722 probes orientated horizontally (TDR_h) and vertically (TDR_v)
723 Figure 8. BEC versus void ratio for a) CH, b) CI and c) CL during consolidation with measurements
724 taken using both TDR_v and TDR_h
725 Figure 9. Relationship between void ratio, e and a) apparent permittivity (AP), b) bulk electric
726 conductivity (BEC) measured in the direction of the load application (v) and normal to the load
727 application (h) during unloading of three CI (CI.S01, CI.S02, CI.S3.TDR) and two CL specimens
728 (CL.S1.TDR, CL.S2.TDR); no unloading was carried out on the CH samples
729 Figure 10. Relative AP_h and AP_v changes (normalised by the pre-loading measurement) in relation to
730 the settlement and the pore pressure dissipation recorded at the top (ps-t), in the middle (ps-m) and
731 at the height of the TDR_h (ps-b). L = loading phase, UL = unloading phase.
732

733 Tables

734 **Table 1. Soil mixtures and index test results**

Soil Mixture	Composition			Index Tests			Activity	Compression	
	ECC	B	S	LL	PL	PI	%	C_c	C_s
	%			%				-	
CH	85	5	10	56	26	30	0.33	0.38	0.08
CI	45	5	50	40	15	25	0.50	0.32	0.05
CL	50	0	50	30	18	12	0.24	0.13	0.03

735

736 **Table 2. Specimen loading details**

Specimen No	Soil	Repetition	Initial GWC	Applied Pressure (kPa)						
				L1	L2	L3	L4	L5	L6	L7
1	CH	S01	60	40	80	160	80	-	-	-
2	CH	S02	63	40	80	-	-	-	-	-
3	CH	S5	84	5	10	20	40	-	-	-
4	CI	S1	42	15	25	35	60	80	5	-
5	CI	S2	45	20	35	60	35	5	100	5
6	CI	S3	45	25	50	100	5	-	-	-
7	CI	S8	47	5	15	-	-	-	-	-
8	CI	S9	70	5	0	-	-	-	-	-
9	CL	S1	29	15	25	50	85	100	5	-
10	CL	S2	32	15	25	50	85	5	-	-

737

738

739

740

741 **Table 3. Initial AP and BEC values (Figure 4) in relation to the plasticity and initial VWC**

Soil Mixture	Index Tests			Initial	TDR response	
	LL	PL	PI	VWC	AP	BEC
		%		%	-	S/m
CH	56	26	30	61	36	0.138
CI	40	15	25	55	32	0.098
CL	30	18	12	44	26	0.015

742

743 **Table 4. Conductivity of the soil mixtures measured with TDR in relation to the pore fluid**
 744 **conductivity - measured with low frequency (11 Hz) ER method**

745

Soil	EC _f *	BEC**	BEC/EC _f
	S/m		%
CH	0.247	0.131	53
CI	0.275	0.099	36
CL	0.041	0.01	25

Notes: * pore fluid collected during the loading process (bulk specimen average)

** soil BEC at the end of the consolidation test (bulk specimen average)

746

747 **Table 5. Cation concentrations observed in pore fluid diluted in HNO₃ (measured using ICP-OES,**
 748 **with detection limits of 0.5 to 200 mg/l)**

Specimen	Ca	Na	Mg	K	S	Si	
	mg/l						
CH.S5.TDR	5.09	>209	3.52	17.88	213.20	1.18	0.42
CI.S2.TDR	7.38	>200	4.95	21.28	307.95	2.33	1.03
CI.S3.TDR	7.37	>200	6.31	12.73	299.09	0.85	1.51
CI.S5.TDR	4.97	>252	4.91	18.96	281.80	0.14	0.99
CI.S7.TDR	5.90	>200	24.18	24.57	317.31	5.87	0.37
CL.S2.TDR	2.95	31.64	<0.5	14.19	18.24	14.14	0.35

749